

SOUTHERN BRAZILIAN JOURNAL OF CHEMISTRY 2021 VIRTUAL CONFERENCE

MOLECULAR MODELING, REACTIVITY PARAMETERS AND SPECTROCHEMICAL STUDIES OF ϵ -CAPROLACTAM AND o-PHENANTHROLINE

LIMA, Francisco José Santos*; PESSOA, Maria José de Oliveira; ARAÚJO, Lucas da Silva; SILVA, Ademir Oliveira da, and PEREIRA, Francisco Claudece.

Universidade Federal do Rio Grande do Norte, Centro de Ciências Exatas, Instituto de Química, Brazil

* Corresponding author
e-mail: limafjs@yahoo.com

Received 12 September 2021; received in revised form 30 September 2021; accepted 15 October 2021

ABSTRACT

In this work, molecular models were obtained, and the reactivity parameters of ϵ -caprolactam and o-phenanthroline were calculated to evaluate the interaction in the formation of complex molecular compounds. It was observed that the main electron donor atoms, in the formation of the metal-ligand bond, are centered mainly on the oxygen and nitrogen atoms, respectively, which are sterically more favorable in these species. Conductance measurements in an aqueous solution were obtained to observe the electrolytic behavior of these compounds. Infrared spectra were also recorded to characterize vibrational transitions in identifying these species when present in complex systems. Molecular spectra of absorption in the UV-visible region were recorded to evaluate the spectrochemical properties of these individual ligands and further verify their influence on the formation of complex molecular systems. The parameters evaluated include the molar absorptivity ϵ , integrated absorption coefficient, oscillator force, and transition dipole moment. It was observed that the ϵ parameter indicates molecular transitions in the 190 – 300 nm region and the near-infrared, and the oscillator strength is typical of molecules used as dyes and sensitizers for optical light-emitting systems or light-to-electricity converters.

Keywords: oscillator strength, transition dipole moment, spectrochemical properties.

1. INTRODUCTION

The ϵ -caprolactam is a cyclic chain amine with molecular formula $C_6H_{11}NO$, molar mass 113.16 g / mol, soluble in water (50 mg / mL), which in aqueous solution has a pH between 7.0 - 8.5 (333 g/L). In the chemical industry, it has been widely used as a precursor of polymers called nylon 6. More recently, it has been applied in the synthesis of polymeric polyamide compounds (Gong and Yang, 2010), in photochemical-photovoltaic-thermochemical systems (CP-PV-T) for the use of high-efficiency full-spectrum solar energy (Fang *et al.*, 2010), as well as its derivatives, (N-methyl- ϵ -caprolactam) in the synthesis of light-emitting compounds (Borges *et al.*, 2016).

O-phenanthroline is a solid, white, organic heterocyclic compound with the molecular formula $C_{12}H_8N_2$, molar mass 180.21 g/mol, and has a solubility of 3.3 g/L (25 °C) in monohydrate form. Although 1,10-phenanthroline is widely used for fast, flexible, and reliable analysis with a high

scientific reputation in research, other applications are found, such as; uses cathodic protective buffer layers as a conventional binder to improve the efficiency of organic solar cells (Sun *et al.*, 2014), in the study of efficacy in the Luminol chemiluminescence system in Fenton reactions (Mitsuhiro *et al.*, 2014), in complex systems with Cu(I) using mixed ligands to amplify luminescent radiative emissions by electron transfer with a high quantum efficiency (Li *et al.*, 2012).

This work developed molecular modeling, calculated the reactivity parameters, obtained molar conductivity measurements, recorded infrared and UV-visible spectra, and calculated the spectrochemical properties related to the oscillator strength and induced dipole moment.

2. MATERIALS AND METHODS

2.1 Molecular Modeling and Reactivity Parameters

Molecular modeling, theoretical reactivity parameters, electrostatic potential cloud, bonding distances, bonding angles, and partial charges were obtained from the WebLab ViewerPro© program. The parameters were calculated using the following expression (Lima *et al.*, 2020):

$$\Re = \frac{\int q_i d\tau}{\sum_{i=1}^n \left| \int q_i d\tau \right|}$$

Eq. 01

2.2 Conductance, Conductivity and Molar Conductivity

Molar conductivity measurements were performed for aqueous solutions of millimolar concentration, using a QUIMIS Q-405 conductivity meter, at a temperature of 25.0 ± 1 °C, after calibration of the cell constant with freshly prepared standard solutions millimolar of NaCl and KCl. The molar conductivity was calculated using the expression below:

$$\Lambda_M = \frac{(L_{sol} - L_{solv}) \cdot Kc \cdot 10^3}{M} = \frac{(k_{sol} - k_{solv}) \cdot 10^3}{M},$$

Eq. 02

2.3 Spectroscopy in the Infrared Region

The infrared spectra of the two samples were recorded in a PERKIN ELMER FRONTIER equipment, in KBr pellets, in the range of 700 – 4000 cm^{-1} and resolution 4 cm^{-1} .

2.4 Spectroscopy in the UV-Visible Region

The UV-vis spectra were recorded in a SHIMADZU UV model spectrophotometer in the range of 200 - 1000 nm, quartz cuvette with 1 cm optical path for aqueous ϵ -caprolactam solutions (1.18×10^{-2} mol L^{-1}), aqueous o-Phenatroline (1.15×10^{-2} mol L^{-1}) and ethanolic o-Phenatroline (1.01×10^{-2} mol L^{-1}). Samples needed to be diluted. The oscillator force f was calculated by Drago's and Figgs method and described methodologies (Lima *et al.*, 2020) according to the expressions:

$$\text{DRAGO: } f = 4,6 \times 10^{-9} \int \epsilon_{(\sigma)} d\sigma \quad \text{Eq. 03}$$

$$\text{FIGGS: } f = 4,32 \times 10^{-9} \int \epsilon_{(\sigma)} d\sigma \quad \text{Eq. 04}$$

$$\text{Area under the absorption band} = \int A_{(\sigma)} d\sigma = A_{\text{máx.}} (1/\lambda_1 - 1/\lambda_2) \quad \text{Eq. 05}$$

The transition dipole moment was obtained by the following equation:

$$\mu_{if} = 8,422 \times 10^{-22} (\text{m s}^{-1/2} \text{C}) \cdot \sqrt{\frac{f}{\nu}} \quad (\text{C m})$$

Eq. 06

3. RESULTS AND DISCUSSION:

3.1 Molecular modeling, obtaining structural data and reactivity parameters.

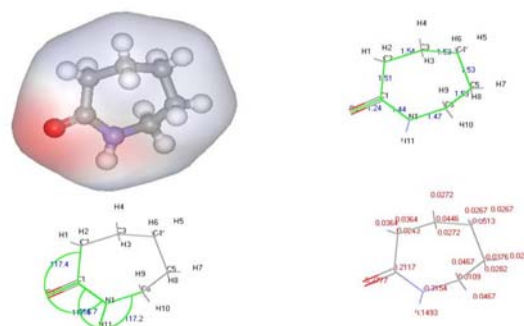


Figure 01 - Modeling obtained for ϵ -Caprolactam, $\text{C}_6\text{H}_{11}\text{NO}$, using the WebLab ViewerPro program©.

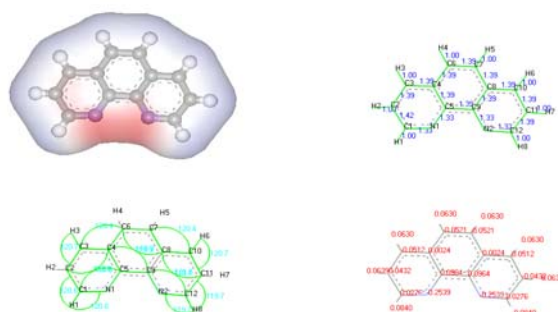


Figure 02 - Modeling obtained for o-Phenanthroline, $\text{C}_{12}\text{H}_8\text{N}_2$, using the WebLab ViewerPro program©.

Table 01 - Partial charges and PRM for ϵ -Caprolactam, $C_6H_{11}NO$. (main atoms)

Atoms	Partial charges		PRM	
	δ^-	δ^+	\mathcal{R}^-	\mathcal{R}^+
O ₁	-0,2777		-0,3822	
C ₁		0,2117		0,2913
H ₁		0,0364		0,0501
H ₁₀		0,0467		0,0643
N ₁	-0,3154		-0,4341	
H ₁₁		0,1493		0,2054

PRM - Molecular Reactivity Parameters

Table 02 - Partial charges and PRM for *o*-Phenanthroline, $C_{12}H_8N_2$. (main atoms)

Atoms	Partial charges		PRM	
	δ^-	δ^+	\mathcal{R}^-	\mathcal{R}^+
C ₁		0,0276		0,0345
C ₁₂		0,0276		0,0345
C ₅		0,0964		0,1204
C ₉		0,0964		0,1204
N ₁	-0,2539		-0,3171	
N ₂	-0,2539		-0,3171	

PRM - Molecular Reactivity Parameters

3.2 Conductivity measurements and the associated electrolyte type.

Table 03 – Conductivities obtained for millimolar aqueous solutions at 25.0 ± 1 °C.

	k $\times 10^{-6}$	M Mol/L	Λ_M	Type of electrolyte
H ₂ O	17,6	55,5	$31,7 \times 10^{-5}$	n-electrol
NaCl	121	0,001	103,4	1:1
KCl	150	0,001	132,4	1:1
ϵ -capro	34,4	0,001	16,8	n-electrol
<i>o</i> -fen	33,0	0,001	15,4	n-electrol

Units: k (S cm^{-1}); Λ_M (S $cm^2 mol^{-1}$)

3.3 Spectra in the infrared region.

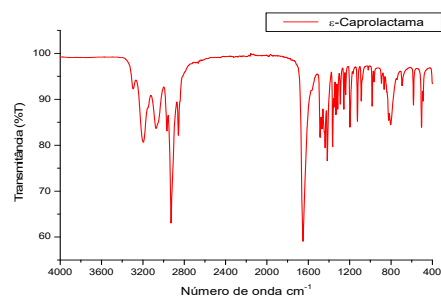


Figure 03 - Infrared spectrum of ϵ -Caprolactam

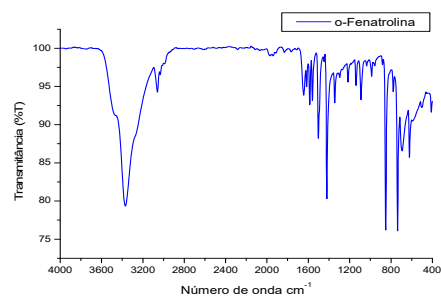


Figure 04 - Infrared spectrum of *o*-Phenanthroline

Table 04 - Vibrational transition assignments for ϵ -Caprolactam (main)

vib. modes	Silverstein 2007	Pavia 2010	Cardoso <i>et al</i> 2017	Exper
N-H	3350 3180	3300 3100		3294 w 3197 m 3073 m
C=O	1720 1706	1680 1630	1663	1652 s
C-N C-N		1400	1461	1467 m 1417 m

w (weak); m (medium); s (strong)

Table 05 - Vibrational transition assignments for *o*-Phenanthroline (main)

vib. modes	Smith, 1961	Martins 2010	Maciel 2015	Exper
$\nu C=N$	1616			1616 m
$\nu_{sim} C=C$			1600	
$\nu C=N$	1585 1558			1586 w 1561 m
νCC	1508			
		1501		1503 s
$\nu C=C$	1418			
νCN		1419		1421 s
C-N _{arom}	1340			1345 w
$\delta C=N$		621		622 m

w (weak); m (medium); s (strong)

3.4 Spectra in the UV-Visible region in aqueous and ethanolic solution.

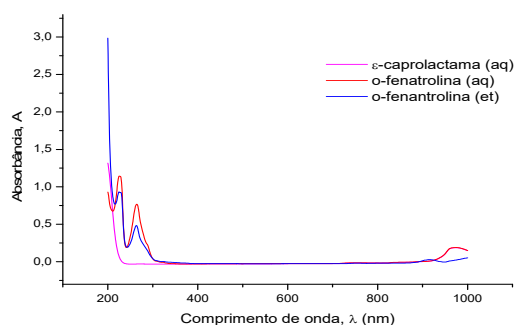


Figure 05 - UV-vis spectrum of ϵ -caprolactam and o-phenanthroline.

Table 07 - Oscillator strength and ligand transition dipole moment.

Ligand	Range Spectral (nm)	f ($\times 10^{-3}$) (adim)		μ_{if} ($\times 10^{-30}$ (C m) (Debye)	
		D	F	D	F
ϵ -cap (aq)	948–999	3,9	3,68	3,0 (0,90)	2,91 (0,872)
o-phe (aq)	948-1000	42	39,2	9,8 (2,9)	9,50 (2,85)
o-phe (et)	900-930	4,5	4,22	3,1 (0,93)	3,22 (0,905)

D – Drago; F – Figgs; 1 Debye = $3,336 \times 10^{-30}$ C m (aq) aqueous solution, (et) ethanolic solution.

4. CONCLUSIONS

Through molecular modeling and reactivity parameters, elements with higher negative densities corroborate that these species function as a Lewis base and act as electron pumpers in certain systems. Conductivity revealed non-electrolyte characteristics. Infrared spectra identified the main vibrational transitions that are identified in the formation of bonds of these species in complex systems. UV-vis spectra show that they do not absorb into the visible, which may be interesting for better use of energy absorption and conversion phenomena, and that the oscillator strength and transition dipole moment reveal that more energetic transitions confirm that they can act as optical pumps and those of lower energy show that their outermost electrons can be delocalized with some ease, and these properties and these ligands can be used in the optimization of light-emitting or electron-transfer systems in light-to-electricity converters.

5. ACKNOWLEDGMENTS

The authors are grateful to the analysis laboratories of IQ UFRN.

6. REFERENCES

- Borges, A. S., Caliman, E. V., Dutra, J. D. L., Silva, J. G. DA, and Araújo, M. H. - *Journal of Luminescence*, V. 170, Part 2, **2016**, 654-662.
- Cardoso, M. C. C.; Belarmino, L. D.; Zukerman-Schpector, J., - *Trabalho apresentado no XLVII Congresso Brasileiro de Química 17 a 21 de setembro*. Disponível em: <http://www.abq.org.br/cbq/2007/trabalhos/2/2-303-504.htm>, **2007**.
- Fang, J., Wu, H., Liu, T., Zheng, Z., Lei, J., Liu, Q., Jin, H. - *Applied Energy*, **2020**, Volume 279.
- Gong, Y., Liu A. Yang, G. - *Composites Part A: Applied Science and Manufacturing* Volume 41, (8), 1006-1011, **2010**.
- Pavia, D. L., Lampman, G. M., Kriz, G. S., Vyvyan, J. R. - *Introdução a Espectroscopia*, **2010**, Cengage Learning Ed., Ltda.
- Li, X. L., Ai, Y. B., Yang, B., Chen, J., Tan., M., Xin, X. L., Shi, Y. H. - *Polyhedron*, **2012**, 35 (1), 47-54.
- Lima, S. G. M.; Cruz, T. J. T.; Pereira, F. C.; Silva, A. O.; Lima, F. J. S. - *Periódico Tche Química*, **2020**, vol. 17(35), 203-215.
- Maciel, J. W O., Vilela-Filho, N. C. - 55^o Congresso Brasileiro de Química, 02 a 06 novembro, Goiânia, GO, **2015**.
- Martins, E. P. S., - *Dissertação de Mestrado, UFPB*, João Pessoa - PB – Brasil, **2010**.
- Mitsuhiro W., Hiroaki K., Rie I., Talal A. A., Suleiman M. A, Naotaka K., and Kenichiro N. - *Luminescence*, **2014**, 29: 955–958.
- Silverstein, R. M.; Webster, F. X.; Kiemle, D. J. - *Identificação Espectrométrica de Compostos Orgânicos*. 7. ed. Rio de Janeiro: Lct, **2007**.
- Smith, R. C. - *Retrospective Theses and Dissertations.*, **1961**, 2419 - <https://lib.dr.iastate.edu/rtd/2419>
- Sun, C., Wu, Y., Zhang W., Jiang, N., Jiu T., and Fang J. - *ACS Appl. Mater. Interfaces*, **2014**, 6, 2, 739–744.